

band and actually has five-fold Pt chain structure⁴. It has a very low conductivity at room temperature as $\sigma_r = 5 \times 10^{-3} \sim 7 \times 10^{-2}$ S/cm and it is also supposed to have a commensurate Peierls structure as α -Rb-OP.

All the partially oxidised platinum complexes with the commensurate Peierls structure are found in POBOP's so far as are summarized in Table 2. Their common features are deduced as follows;

- (1) $k_F = \frac{n-1}{n} \cdot \frac{\pi}{d_{Pt-Pt}}$, where the Pt chain is n-fold.
- (2) The room temperature conductivity σ_r is three to five order of magnitude less than that of the incommensurate salts of the same series.
- (3) Averaged Pt-Pt separation \bar{d}_{Pt-Pt} is relatively short compared with other compounds of this series with commensurate lattice modulation.

The first feature is the condition for the commensurability itself and the second one is the consequence of the above condition. The third one is the structural aspect of the commensurate Peierls structure where the individual Pt-Pt separation in the chain is supposed to be much deviated from the averaged one. This supposition is the structural expression of the second feature. From the point of view of the band

theory, the big conductivity drop is explained as the consequence of the opening of a band gap at the Fermi surface as illustrated in Figure 3-b.

The further structural investigation of Pt spine is very desirable for these compounds to prove the present supposition about their strong bond alternation.

References

1. R.E. Peierls, "Quantum Theory of Solids" Oxford University Press, London 108 (1955).
2. R. Comes, M. Lambert, H. Launois and H.R. Zeller, *Phys. Rev.* **B8** 571 (1973).
3. A. Kobayashi, Y. Sasaki and H. Kobayashi, *Bull. Chem. Soc. Jpn.* **52** 3682 (1979).
4. M. Mizuno, A.E. Underhill and K. Carneiro, *J. Chem. Soc. Dalton Trans.* 1771 (1983).
5. Preliminary results was reported in Abstract of International Conference on Science and Technology of Synthetic Metals, ICSM'86 Kyoto, 454 (1986).
6. O. Bekaroglu, M. El Sharif, H. Endres and H.J. Keller, *Acta Cryst.* **B32** 2983 (1976).

Lewis Acid Catalysis of Coumarin and 5,7-Dimethoxycoumarin Photodimerization

Sang Chul Shim*, Eun Il Kim, and Ki Taek Lee

*Department of Chemistry, Korea Advanced Institute of Science and Technology,
Seoul 131. Received December 23, 1986*

The effect of Lewis acids on spectroscopic properties and photodimerization of coumarin and 5,7-dimethoxycoumarin was investigated. Quantum yields of coumarin photodimerization increase in the presence of $\text{BF}_3 \cdot \text{OEt}_2$ but those of 5,7-dimethoxycoumarin decrease. The spectroscopic properties of the coumarin- $\text{BF}_3 \cdot \text{OEt}_2$ and 5,7-dimethoxycoumarin- $\text{BF}_3 \cdot \text{OEt}_2$ complexes were studied by UV, IR, ^1H NMR and fluorescence spectroscopy.

Introduction

Lewis acids have been widely employed as catalysts for thermal Diels-Alder and ene reactions, especially those involving α, β -unsaturated esters.¹ The enhanced reactivity and stereoselectivity observed in many such reactions have been attributed to changes in frontier orbital energies and double bond polarity upon complexation of the carbonyl oxygen.²

The possibility that Lewis acid might serve as a catalyst for photochemical reactions have been recognized for many years, and the recent literature offers increasing number of reports about photochemical reactions accelerated by Lewis acids.

It is reported that the spectroscopic properties and unimolecular photoisomerization reactions of several α, β -unsaturated esters are profoundly changed by complexation with Lewis acids such as BF_3 , EtAlCl_2 and SnCl_4 .³⁻⁶ Irradiation of several α, β -unsaturated esters in the presence of Lewis acids leads to photostationary states enriched in the thermodynamically less stable *cis* isomer.³ From a mech-

anistic standpoint, selective *trans-cis* photoisomerization occurred via complexation of ester carbonyl oxygen with Lewis acids.⁵ Such a complexation changes spectroscopic properties resulting in selective *trans-cis* photoisomerization upon irradiation of the ground state ester-Lewis acid complexes.

Lewis acids have also served as a catalyst for photochemical [2+2] cycloaddition reactions such as photodimerization of *trans,trans*-dibenzylidenacetone in the presence of UO_2^{2+} and SnCl_4 ,^{7,8} and photodimerization of coumarin and cinnamate esters in the presence of $\text{BF}_3 \cdot \text{OEt}_2$.^{9,10}

To explain the effects of Lewis acids on [2+2] photocycloaddition reactions and possible role of Lewis acid catalysts in photochemical reactions, we investigated spectroscopic properties and photodimerization reactions of coumarin(I) and 5,7-dimethoxy-coumarin (DMC,II) in the presence and absence of Lewis acids.

Experimental

Materials. 5,7-Dimethoxycoumarin (Aldrich) was recrystallized.

stallized from ethanol twice. Coumarin (Eastman) and boron trifluoride etherate (Aldrich) were used as received. HPLC grade dichloromethane, n-hexane, and tetrahydrofuran were used for high performance liquid chromatography. Ethyl ether was refluxed over sodium and distilled prior to use. Dichloromethane was distilled from phosphorous pentoxide and other common solvents were used without further purification. Kiesel Gel GF₂₅₄ (Merck) and Kiesel Gel 60 (70-230 mesh) (Merck) were used for silica gel thin layer chromatography and column chromatography, respectively.

Spectra. Ultraviolet-visible spectra were recorded on a Cary-17 spectrophotometer. Infrared spectra were measured on a Perkin-Elmer 267 spectrophotometer (potassium bromide pellet). ¹H NMR spectra were obtained on a Varian FT-80A NMR spectrometer in chloroform-d. Mass spectra were obtained on a Hewlett Packard 5985A GC/MS system using electron impact (EI) method. Fluorescence spectra were recorded on an Aminco-Bowman spectrofluorimeter with Aminco-XY recorder. High performance liquid chromatogram was obtained on a Waters Associates Model 244 liquid chromatograph equipped with Model 6000A solvent delivery system and Model 440 UV detector (254 nm and 280 nm).

Quantum Yield Measurements. Samples for quantum yield determination were degassed and sealed in Pyrex ampoules. Sample solutions (3 ml) were pipetted into ampoules, degassed through three to five cycles of freeze-pump-thaw method with cooling in liquid nitrogen and sealed. The samples were irradiated with Hanovia 450 W medium-pressure mercury arc lamp (Type 679A36) in a merry-go-round apparatus. Mercury emission line of 366.0 nm was isolated by Corning glass filters #0-52 and #7-37. Ferrioxlate actinometry was used to monitor the intensity of the light absorbed.¹¹ Quantitative analysis was carried out by HPLC techniques. The following conditions are used for coumarin and 5,7-dimethoxycoumarin dimerization quantitative analysis: column; μ -porasil (3.9 mm I.D \times 30 cm), solvents; n-hexane/ethyl ether (1/2, v/v), flow rate; 1.7 ml/min and n-hexane/dichloromethane/tetrahydrofuran (200/100/5, v/v), flow rate; 2.0 ml/min, detector UV (254 nm).

Preparation of Lewis Acid Complexes and Photodimers of Coumarin and 5,7-Dimethoxycoumarin. Coumarin-BF₃·OEt₂ and DMC-BF₃·OEt₂ complexes were prepared by addition of excess BF₃·OEt₂ into CCl₄ solutions of coumarin and DMC. The resulting precipitate was collected by filtration and dried in vacuum. Coumarin *syn* head-to-tail dimer was synthesized as reported in the literature.⁹ 5,7-Dimethoxycoumarin *syn* head-to-tail and *anti*-dimer were also prepared by the literature method.¹²

Results and Discussion

Addition of a small amount of BF₃·OEt₂ to DMC solution causes a reduction in the 325 nm absorption band and a shoulder at 360 nm appears as shown in Figure 2. The isosbestic point at 340 nm is indicative of incomplete complexation showing the light absorption by both free and complexed DMC. The 325 nm band disappeared and a new band at 366 nm is observed on addition of excess BF₃·OEt₂ probably due to the complete complexation of DMC with BF₃·OEt₂. The results eliminate the possibility of complexation of Lewis acids on methoxy oxygen since it would cause a

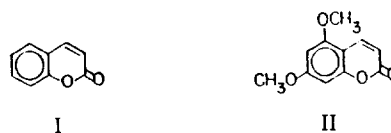


Figure 1. Structure of coumarin (I) and 5,7-dimethoxycoumarin (DMC, II).

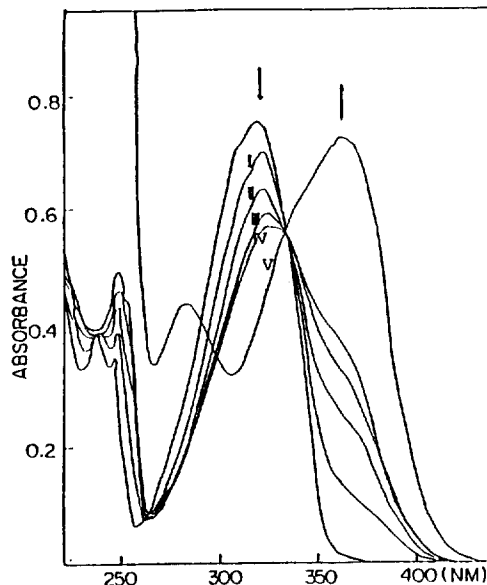


Figure 2. UV spectra of 5,7-dimethoxycoumarin (4.7×10^{-5} M) in the absence and presence of 5.0×10^{-3} (I), 1.0×10^{-2} (II), 1.5×10^{-2} (III), 2.0×10^{-2} (IV), 0.38 M (V) BF₃·OEt₂.

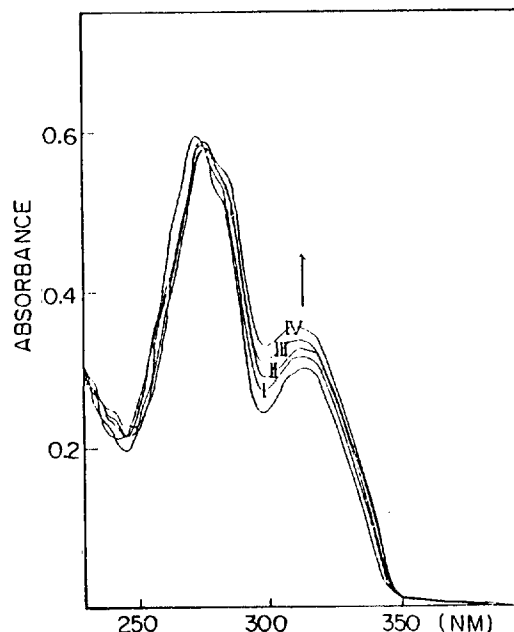


Figure 3. UV spectra of coumarin (5.0×10^{-5} M) in the absence and presence of 5.0×10^{-3} (I), 1.0×10^{-2} (II), 1.5×10^{-2} (III), 2.0×10^{-2} (IV) M BF₃·OEt₂.

blueshift in contrast to the observed red-shift. The absorption spectra of coumarin in the absence and presence of BF₃·OEt₂ are shown in Figure 3. As the concentration of BF₃·OEt₂ increased, the intensity of 313 nm band increased

a little but no new peak or shoulder appeared at the longer wavelength. The results indicate that the properties of each complex-formed are different and the equilibrium constant for complexation is not large.

The ^1H NMR data for the coumarin, DMC and their complexes with $\text{BF}_3 \cdot \text{OEt}_2$ in CDCl_3 solution are summarized in Table 1. The vinyl proton resonance peaks of the pyron ring in both DMC and coumarin are downfield shifted by 1.0 equiv. $\text{BF}_3 \cdot \text{OEt}_2$ indicating that coumarin and $\text{DMC} \cdot \text{BF}_3 \cdot \text{OEt}_2$ complexes change the environments of 3,4-double bond in both compounds. But only minor change was observed in the $J_{\alpha, \beta}$ coupling constant.

Table 1. ^1H NMR Data for 5,7-Dimethoxycoumarin and Coumarin and Their Lewis Acid Complexes^a

compounds	Lewis acid	chemical shift, ppm		$^3J_{\alpha, \beta}$ (Hz)
		H_α	H_β	
5,7-DMC		7.91	6.11	9.6 ^c
5,7-DMC	$\text{BF}_3 \cdot \text{OEt}_2$	8.25	6.47	9.8
Coumarin		7.60	6.31	9.1
Coumarin	$\text{BF}_3 \cdot \text{OEt}_2$	7.78	6.50	9.3

^aChemical shifts for 0.1 M 5,7-dimethoxycoumarin and coumarin in CDCl_3 vs. TMS in the absence or presence of 1.0 equivalent of Lewis acid.

One equiv. $\text{BF}_3 \cdot \text{OEt}_2$ is not enough for complete complexation as shown in the UV study and the chemical shifts observed are time average of those of the complexed and free coumarin and DMC.

The downfield shift of vinyl proton peaks in DMC is larger than that of coumarin indicating the stronger complexation in DMC probably due to the strong electron donating ability of methoxy groups making the following charge transfer resonance structure II contribute to the complexation of DMC with $\text{BF}_3 \cdot \text{OEt}_2$. (Figure 4)

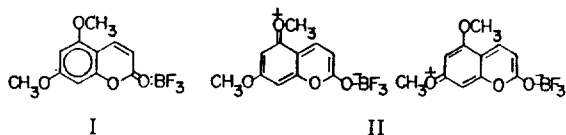


Figure 4. A plausible structure of $\text{DMC} \cdot \text{BF}_3 \cdot \text{OEt}_2$ complex.

In infrared spectra, DMC carbonyl stretching vibration at 1710 cm^{-1} is shifted to 1690 cm^{-1} in the complex. Also a new broad band appeared at $1040\text{--}1180 \text{ cm}^{-1}$ possibly due to $\text{O} \rightarrow \text{B}$ vibration.¹³ The 20 cm^{-1} red-shift of the complexed carbonyl stretching band strongly indicates that BF_3 is linked to the carbonyl oxygen. Coumarin carbonyl stretching band is not shifted but a new broad band appeared at $1040\text{--}1180 \text{ cm}^{-1}$ suggesting that carbonyl oxygen of coumarin does not strongly interact with BF_3 as compared with that of DMC.

The DMC fluorescence intensity ($\lambda_{\text{max}} = 400 \text{ nm}$) decreases and a new peak ($\lambda_{\text{max}} = 465 \text{ nm}$) appears at the longer wavelength with increasing $\text{BF}_3 \cdot \text{OEt}_2$ concentration as shown in Figure 5. A new peak at the longer wavelength is probably due to the excited states of the complex formed between DMC and $\text{BF}_3 \cdot \text{OEt}_2$. The excitation spectra shown in Figure 6 confirm that each fluorescent species is different substance. As the concentration of $\text{BF}_3 \cdot \text{OEt}_2$ is increased,

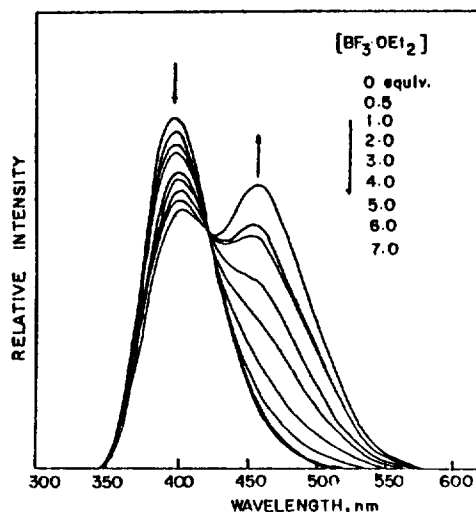


Figure 5. Fluorescence emission spectra of 5,7-dimethoxycoumarin ($5.0 \times 10^{-5} \text{ M}$) in the absence and presence of 0.5, 1, 2, 3, 4, 5, 6, 7 equiv. $\text{BF}_3 \cdot \text{OEt}_2$ ($\lambda_{\text{ex}} = 325 \text{ nm}$).

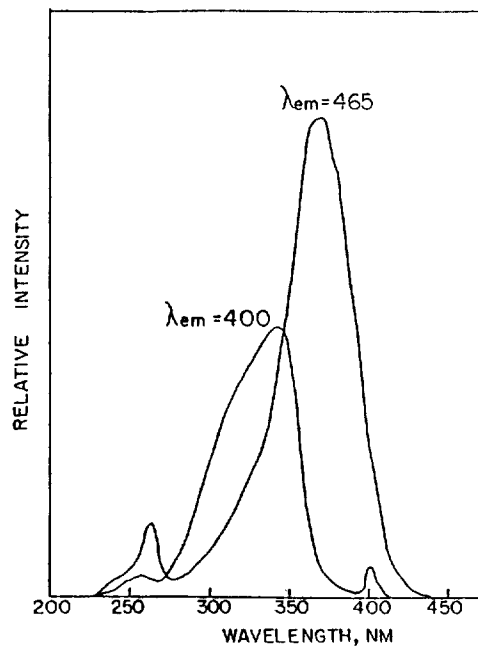


Figure 6. Fluorescence excitation spectra of 5,7-dimethoxycoumarin ($5.0 \times 10^{-5} \text{ M}$) in the presence of 5.0 equiv. $\text{BF}_3 \cdot \text{OEt}_2$.

the fluorescence quenching of DMC is more efficient. A variety of processes can result in quenching.¹⁴ Collisional or dynamic quenching can result from collisional encounters between the fluorophore and quencher. But static quenching is due to the ground state complexation. Collisional quenching affects the excited state of fluorophores, and thus no change in the absorption spectra is predicted. In contrast, ground state complexation frequently results in perturbation of the absorption spectrum. UV spectra of DMC in the presence of $\text{BF}_3 \cdot \text{OEt}_2$ is red-shifted. Therefore, the fluorescence quenching of DMC by the formation of ground state complex is a static quenching process.

As the concentration of $\text{BF}_3 \cdot \text{OEt}_2$ increased, the fluorescence intensity ($\lambda_{\text{ex}} = 315 \text{ nm}$) is greatly increased in coumarin as shown in Figure 7. It has already been reported

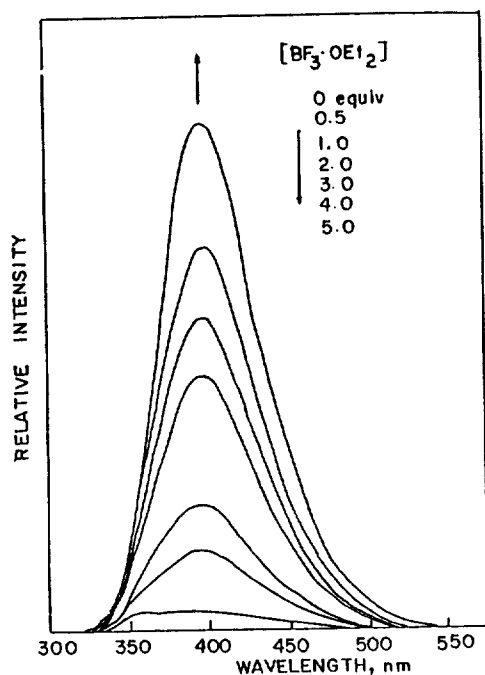


Figure 7. Fluorescence emission spectra of coumarin ($5.0 \times 10^{-5} \text{M}$) in the absence and presence of 0.5, 1, 2, 3, 4, 5 equiv. $\text{BF}_3 \cdot \text{OEt}_2$ ($\lambda_{\text{ex}} = 315 \text{nm}$).

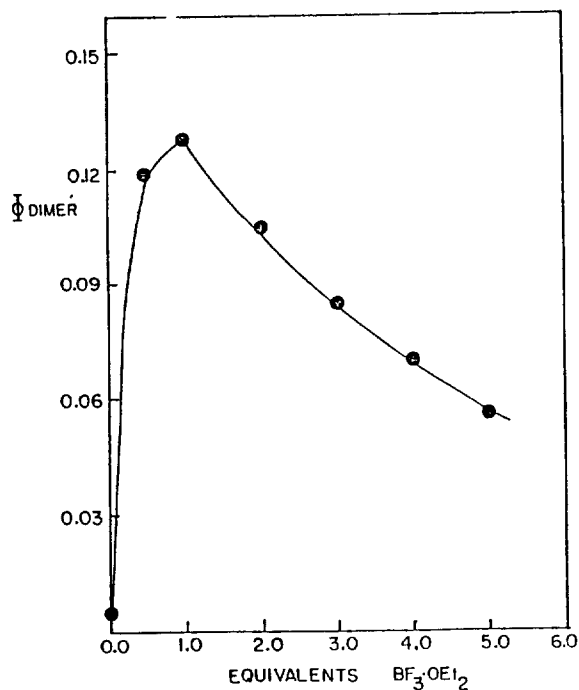


Figure 8. Quantum yields for photodimerization of coumarin (0.2 M) in the absence and presence of 0.5, 1, 2, 3, 4, 5 equiv. $\text{BF}_3 \cdot \text{OEt}_2$.

that the coordination of the positive lithium ion with coumarin carbonyl group enhances the fluorescence quantum yield and life time.¹⁵ These results are due to a weakening of the vibronic interaction between the $^1(n, \pi^*)$ and $^1(\pi, \pi^*)$ states, as the $^1(n, \pi^*)$ state is elevated to higher energy by the lithium ion coordination. The enhanced fluorescence intensity of coumarin can be explained in the same manner. Lewis acid complexation lowers the energy of the oxygen nonbonding

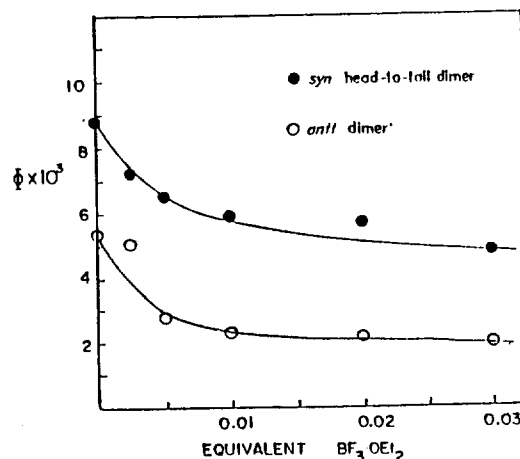
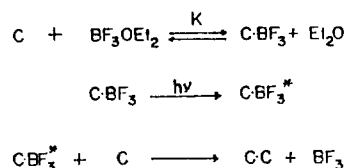


Figure 9. Quantum yields for photodimerization of 5,7-dimethoxycoumarin (0.02 M) in the absence and presence of 0.0025, 0.005, 0.01, 0.02, 0.03 equiv $\text{BF}_3 \cdot \text{OEt}_2$.

electrons hence raises the energy of the $^1(n, \pi^*)$ state relative to the $^1(\pi, \pi^*)$ state.

The effect of $\text{BF}_3 \cdot \text{OEt}_2$ on coumarin photodimerization quantum yield is summarized in Figure 8. The dimerization quantum yields increase from 10^{-3} with coumarin alone to 0.13 with 1.0 equiv. of $\text{BF}_3 \cdot \text{OEt}_2$ and decrease at higher $\text{BF}_3 \cdot \text{OEt}_2$ concentration. This supports the reaction of excited coumarin- $\text{BF}_3 \cdot \text{OEt}_2$ complex with ground state coumarin for dimerization since extensive complexation will lower the free coumarin concentration and consequently the dimerization quantum yield.

The enhanced quantum yield for coumarin photodimerization in the presence of $\text{BF}_3 \cdot \text{OEt}_2$ can be attributed to increase of concentration of coumarin- $\text{BF}_3 \cdot \text{OEt}_2$ complex which has more reactive excited state than coumarin alone. Both UV absorbance and fluorescence intensity of coumarin increase greatly with increasing $\text{BF}_3 \cdot \text{OEt}_2$ concentration. The vibronic interaction between the $^1(n, \pi^*)$ and $^1(\pi, \pi^*)$ states is reduced due to the complexation and the lowest excited state of coumarin- $\text{BF}_3 \cdot \text{OEt}_2$ complex is closer to pure $^1(\pi, \pi^*)$ state. Since the photoreactivity of coumarin is determined by the electronic structure of the lowest excited states (S_1), almost pure (π, π^*) character of the lowest excited state makes the coumarin- $\text{BF}_3 \cdot \text{OEt}_2$ complex more reactive than coumarin alone. A plausible mechanism for the $\text{BF}_3 \cdot \text{OEt}_2$ promoted photodimerization of coumarin is outlined in scheme 1.



Scheme 1

In contrast to coumarin, no DMC dimer formation was observed in the presence of highly concentrated $\text{BF}_3 \cdot \text{OEt}_2$ and the dimerization quantum yields decreased on addition of very small amounts of $\text{BF}_3 \cdot \text{OEt}_2$ (Fig. 9) in spite of increasing fluorescence intensity of DMC- $\text{BF}_3 \cdot \text{OEt}_2$ complex (Fig. 5). UV absorption of DMC- $\text{BF}_3 \cdot \text{OEt}_2$ complex also increased

as in the case of coumarin but λ_{max} is very much red-shifted suggesting that DMC-BF₃·OEt₂ complexation extends conjugation, probably resonance interaction between methoxy groups and BF₃ as shown in Fig. 4. The large contribution of resonance structure (II) may inhibit the photodimerization reaction because the 3,4-double bond character of DMC-BF₃·OEt₂ complex is greatly decreased by BF₃·OEt₂ complexation and photodimerization quantum yields decrease with increasing BF₃·OEt₂ concentration.

In conclusion, an increase or decrease of the photodimerization efficiency of coumarin and DMC on addition of BF₃·OEt₂ are not due to acceleration of the reaction rate of the excited states involved, but to complexation between the ground state of the compounds and BF₃·OEt₂ prior to excitation.

Acknowledgements. This investigation was supported by US PHS Grant Number 5 R01 CA 212729, awarded by the National Cancer Institute, DHHS, USA and by the Korea Science and Engineering Foundation Grant.

Reference

1. I. Fleming, "Frontier Orbitals and Organic Chemical Reactions", Wiley, New York, 1976, pp 214-223.
2. K.N. Houk and R.W. Strozier, *J. Am. Chem. Soc.*, **95**, 4094 (1973).
3. F.D. Lewis and J.D. Oxman, *J. Am. Chem. Soc.*, **103**, 7345 (1981).
4. F.D. Lewis, J.D. Oxman, L.L. Gibson, H.L. Hampsch and S.L. Quillen, *J. Am. Chem. Soc.*, **108**, 3005 (1986).
5. F.D. Lewis, D.K. Howard, S.V. Barancyk and J.D. Oxman, *J. Am. Chem. Soc.*, **108**, 3016 (1986).
6. F.D. Lewis, D.K. Howard, J.D. Oxman, A.L. Upthagrove and S.L. Quillen, *J. Am. Chem. Soc.*, **108**, 5964 (1986).
7. N.W. Alcock, N. Herron, T.J. Kemp and C.N. Shoppe, *J. Chem. Soc., Chem. Commun.*, 785 (1975).
8. P. Praetorius and F. Korn, *Ber.*, **43**, 2774 (1910).
9. F.D. Lewis, D.K. Howard and J.D. Oxman, *J. Am. Chem. Soc.*, **105**, 3344 (1983).
10. F.D. Lewis and J.D. Oxman, *J. Am. Chem. Soc.*, **106**, 466 (1984).
11. C.G. Hatchard and C.A. Parker, *Proc. Roy. Soc. (London) A* **235**, 518 (1956).
12. S.C. Shim, K.Y. Choi and P.-S. Song, *Photochem. Photobiol.*, **27**, 25 (1978).
13. R.C. Paul and S.L. Chadha, *Aust. J. Chem.*, **22**, 1381 (1969).
14. J.R. Lakowich, "Principles of Fluorescence Spectroscopy," Plenum Press, New York.
15. P.-S. Song and Q. Chae, *J. Luminesc.*, 12/13, 831 (1976).

Comparing the Stability of Geometrically rigid Tricyclopropyl Carbinyl Cations by ¹⁹F NMR Spectroscopy

Jung-Hyu Shin*, Kyongtae Kim, and Hun-Woo Shin

Department of Chemistry, Seoul National University, Seoul 151. Received January 13, 1987

The relative stability as function of geometry in the rigid tricyclopropylcarbinyl cations with varied bond angle (α) between the plane of cyclopropane ring and the bond connecting cyclopropane ring to cationic carbon was examined by ¹⁹F nmr spectroscopy. 7-p-Fluorophenyltricyclo[2.2.2.0^{2,6}]octan-7-yl (**4**) and 8-p-fluorophenyltricyclo[3.2.2.0^{2,7}]nonan-8-yl cation (**8**) were generated from corresponding tertiary alcohols under stable ion conditions, and their ¹⁹F chemical shifts were compared with those of model compounds such as 7-nortricyclyl cation (**3**) and tricyclo[3.3.1.0^{2,7}]octan-8-yl cation (**7**). Consequently, it is concluded that the varied orientation of bond angle (α) within in the bisected conformation does not affect degree of the charge delocalization into cyclopropane ring.

Among neighboring groups which provide stabilization to adjacent carbocationic center, the effectiveness of the cyclopropyl group is well documented.¹ The very large conjugative interaction between a strained cyclopropane bonds and adjacent empty or developing p orbital has been the object of continuing wide interest. The "bisected" conformation (**1**, $\theta = 0^\circ$) of a cyclopropyl cation is energetically favored over the "perpendicular" one (**2**, $\theta = 90^\circ$) by about

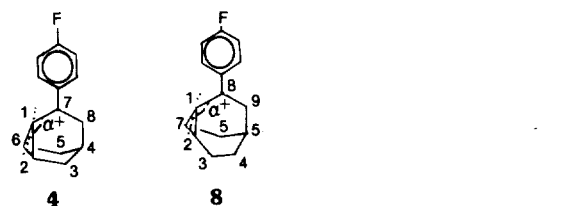
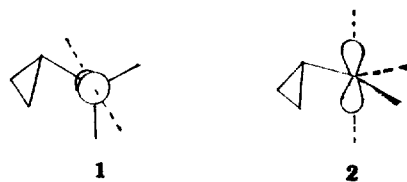


Figure 1

16 kcal/mol.² Recently, it has been demonstrated that a cyclopropylcarbinyl cation is also stabilized when the conformation of the system is locked by structural constraints at an intermediate position between bisected and perpendicular conformation.³ Indeed, the change in energy of a cyclopropylcarbinyl cation upon rotation of the cation center